

# Half metallic state and magnetic properties versus the lattice constant in $Ti_2CoSn$ Heusler compound: an ab initio study.

A. Birsan<sup>a</sup>, P. Palade<sup>a</sup>, V. Kuncser<sup>a</sup>

<sup>a</sup>National Institute of Materials Physics, PO Box MG-07, Bucharest, Romania

---

## Abstract

The half metallic properties of  $Ti_2CoSn$  full-Heusler compound is studied within the framework of the density functional theory with the Perdew Burke Ernzerhof generalized gradient approximation (GGA). Structural optimization was performed and the calculated equilibrium lattice constant is 6.340 Å. The spin up band of compound has metallic character and spin down band is semiconducting with an indirect gap of 0.598 eV at equilibrium lattice constant. For the lattice parameter, ranging from 6.193 to 6.884 Å the compound presents 100% spin polarization and a total magnetic moment of  $3\mu_B$ .

**Keywords:** A.  $Ti_2CoSn$ ; B. Density of states theory; C. Electronic structure; D. Magnetic properties.

---

## 1. Introduction

Discovered in 1903, when Fritz Heusler found that the composition  $Cu_2MnAl$  behaves like a ferromagnet Heusler et al. (1903); Heusler (1903), Heusler alloys are half-metallic ferromagnets, semiconducting for electrons of one spin orientation and metallic character for electrons with the opposite spin orientation. These materials attracted remarkable attention because of the magnetic behavior or multifunctional magnetic properties, like magneto-optical van Engen et al. (1983), magneto-structural characteristics Kainuma et al. (2006) and nearly fully spin polarized conduction electrons, suitable for spintronic applications. Divided in two distinct families these ternary semiconducting or metallic materials have the general formula  $XYZ$  or  $X_2YZ$  with 1:1:1 (half-Heusler, ) or 2:1:1 (full-Heusler ) stoichiometry. The crystalline structure typical for half-Heusler materials is the non-centrosymmetric cubic structure  $C1_b$  Heusler et al. (1903); Heusler (1903); Webster et al. (1988), while full-Heusler alloys crystallize in the cubic space group with  $Cu_2MnAl$  ( $L2_1$ ) prototype Heusler et al. (1903); Heusler (1903); Webster et al. (1988) or  $Hg_2CuTi$  prototype, if the number of 3d electrons of  $Y$  atom exceeds that of  $X_2$  atom Kandpal et al. (2007). In the last decades,  $Mn_2$ ,  $Co_2$ ,  $Fe_2$  or  $Cr_2$  -based Heusler alloys have been widely studied Buschow et al. (1981); Chen et al. (2006); Kumar et al. (2010); Graf et al.

(2011); Weht et al. (1999); Ozdogan et al. (2006); Fecher et al. (2006); Galanakis et al. (2007); ZhongyuYao et al. (2010); Luo et al. (2007); Li et al. (2009), however only few of  $Ti_2$ -based full Heusler alloys were investigated Kervan et al. (2012); Pugaczowa-Michalska Maria (2012); Kervan et al. (2011); Lei et al. (2011). In the present paper, the half metallic properties of  $Ti_2CoSn$  are theoretically investigation by first-principles calculations of density of states, energy bands, and magnetic moments. The purpose is to analyze if the half-metallicity reported in  $Ti_2CoB$  Kervan et al. (2011),  $Ti_2CoGe$  Huang et al. (2012) and  $Ti_2CoZ$  ( $Z=Al, Ga, In$ ) Bayar et al. (2011); Kervan et al. (2011, 2012); Wei et al. (2012); Zheng et al. (2012) is destroyed by the substitution of  $B, Ge, Al, Ga$  or  $In$  with  $Sn$  atoms.

## 2. METHOD OF CALCULATION

Geometric optimization and the electronic structure calculations, based on the density functional theory (DFT) were performed by means the self consistent full potential linearized augmented plane wave (FPLAPW) method implemented in Wien2k code Blaha et al. (2009). For the exchange and correlation interaction was used the Perdew Burke Ernzerhof Perdew et al. (1996) generalized gradient approximation (GGA) where the interstitial region employed Fourier series and for muffin-tin sphere, spherical harmonic functions. The plane wave cut-off value used was  $K_{max}R_{MT} = 7$ , where  $K_{max}$  is the maximum modulus for the reciprocal lattice vector. The muffin-tin (MT) sphere radii selected for Ti, Co and Sn were 2.33, 2.33 and 2.35 a.u. respectively. The integration over the irreducible part of the Brillouin zone (BZ), using the energy eigenvalues and eigenvectors of a grid containing 2925k points, was done using the modified tetrahedron method Blöchl et al. (1994). The selected convergence criteria during self-consistency cycles considered was an integrated charge difference between two successive iterations less than 0.0001e/a.u.<sup>3</sup> and the total energy deviation better than 0.01mRy per cell.

## 3. RESULTS AND DISCUSSIONS

The structure of  $Hg_2CuTi$  prototype was used to define the unit cell of  $Ti_2CoSn$  compound, because Ti element is less electronegative than Co element. In this structure, exhibited in Fig.1, the Wyckoff positions 4a, (0 0 0) and 4c, (1/4 1/4 1/4) are occupied by Ti element, which makes them nearest neighbors, whereas Co and Sn occupy the 4b, (1/2 1/2 1/2) and 4d, (3/4 3/4 3/4) positions. The inversion symmetry typical for  $L2_1$  structure with  $Fm\bar{3}m$  is broken, and it is assigned to  $F\bar{4}3m$  space group. Therefore, the  $Hg_2CuTi$  prototype, also called inverse Heusler structure can be thought of as a generalization of  $L2_1$ , which is the typical Heusler structure. The GGA parameterization with non-magnetic, antiferromagnetic and spin polarized ferromagnetic setup were employed for structural optimization, within the FLAPW-scheme. The superstructure constructed to be used for these configurations, resulted from spreading the unit cell crystal structure along the axis of  $a$  lattice parameter

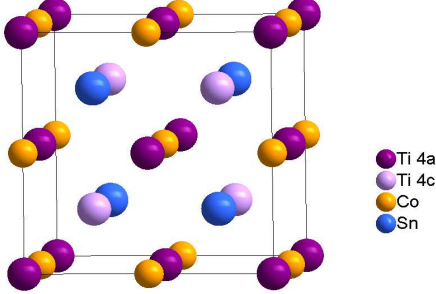


Figure 1: The unit cell structure of  $Ti_2CoSn$  compound has  $Hg_2CuTi$  prototype.

and contains an even number of  $Co$  atoms with nearest-neighbor spins, oriented in opposite directions. Geometrical optimization, plotted in Fig.2 was performed to determine the lattice parameter which minimizes the total energy. The iteration procedure for each of the different lattice parameter was performed up to self-consistency. In the non-magnetic and antiferromagnetic cases, the minimum total energies were found to be higher than that found for ferromagnetic (spin-polarized) configuration. The optimized lattice constant found for  $Ti_2CoSn$  compound is 6.34 Å, in ferromagnetic phase and no experimental or theoretical value are available in literature, to compare with our results.

The spin-projected total densities of states (DOS) and partial DOSs(PDOS) of  $Ti_2CoSn$  obtained by performing the spin-polarized calculations at equilibrium lattice constant are displayed in Fig. 3. The majority spin channel (spin-up band) presents a clear metallic character while the minority spin channel (spin-down band) is semiconducting with a energy gap around the Fermi level. Additionally are exhibited the main partial densities of states of Ti, Co and Sn atoms, where 4c, 4a, 4b and 4d represent the Wyckoff positions from crystal structure. It is worth to be noted, that between -2 eV and -1 eV the energy comes mainly from d electrons of Co atoms. Between -5.5 eV and -2.5 eV the significant contribution comes from p electrons of Sn.

At equilibrium lattice constant the Fermi level is located at 0.393 eV from the triple degenerated occupied Ti(4c)  $d_{t2g}$  (below  $E_F$ ) and at 0.151 eV from unoccupied Ti(4a) and Ti (4c)  $d_{t2g}$  states (above  $E_F$ ) as has been plotted in Fig 4. Therefore, the energy gap is clearly formed due to Ti-Ti hybridization, by splitting d states of Ti atoms, located in the two different Wyckoff positions in the minority spin channel. The 3d orbitals of Co are fully occupied and form a weak covalent interaction with Ti 3d orbitals.

In Fig 5 is plotted the band structure of  $Ti_2CoSn$  compound at equilibrium geometry. The width of the indirect band gap of 0.598 eV is calculated using the energy of the highest occupied band at the G point (0.420 eV) and the lowest unoccupied band at L point (0.178 eV), from the spin-down band structure.

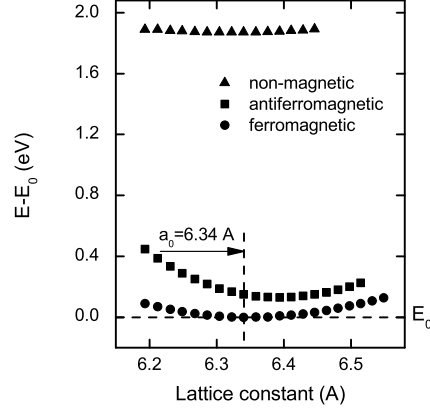


Figure 2: Structural optimization for  $Ti_2CoSn$ . - The change of calculated total energy as function of the lattice constant is displayed. The non-magnetic, antiferromagnetic and spin polarized ferromagnetic configurations are compared. For better comparison, all energy scales are shifted to  $E(0)=0$  eV.

The bandstructure reveals that Ti-Ti bonding interactions are the strongest, even though Ti-Co interactions also play a role. The size of the gap, related to the difference in energy, between the bonding and antibonding  $d$  states it is larger than the reported energy gap for all  $Ti_2Ni$ ,  $Ti_2Fe$ ,  $Ti_2Mn$ -based compounds studied Lei et al. (2011); Kervan et al. (2011); Wei et al. (2012); Zheng et al. (2012). The substitution of  $B$ ,  $In$  or  $Ge$  with  $Sn$  in  $Ti_2Co$ -based compounds, leads to a decrease of minority band gap Kervan et al. (2012, 2011); Huang et al. (2012) at reported optimized lattice constants but doesn't destroy the half metallic character. For  $Ti_2CoAl$  compound, the size of energy gap from minority spin channel reported by Wei et al. (2012) (0.68 eV) is significantly larger than those calculated by other authors: 0.49 eV Bayar et al. (2011) and 0.486 eV Zheng et al. (2012). A similar situation was found for  $Ti_2CoGa$  when the sizes of the minority band gaps were 0.5 eV Kervan et al. (2012) and 0.68 eV Wei et al. (2012). In this context, further investigations are needed to clarify the width of band gaps from minority spin channel in the  $Ti_2CoZ$  compounds with  $Z=Al$  or  $Ga$ .

Fig. 6 shows the calculated values for total spin magnetic moment  $M_{tot}^{calc}$  ( $\mu_B/f.u.$ ) and spin magnetic moment of each atom  $M^{calc}$  ( $\mu_B/atom$ ) as function of lattice parameter. The total magnetic moment is equal to  $3 \mu_B$ , following the rule  $M_t = Z_t - 18 \mu_B/f.u.$  Zheng et al. (2012) ( $M_t$  is the total spin magnetic moments per formula unit cell and  $Z_t$ , the total number of valence electrons) and starts decreasing for a lattice constant above 6.884 Å. In the lattice parameter interval where the total spin magnetic moment is constant, the spin magnetic moments of Ti (4a), Co and Sn decrease with increasing of lattice constant, while the magnetic moment of Ti (4c) increases. The spin-polarization calculations

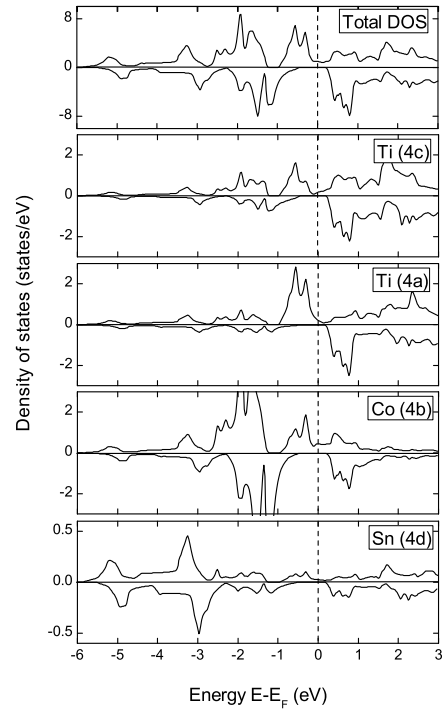


Figure 3: Spin-projected total densities of states (DOS) and partial DOSs calculated at predicted equilibrium lattice constant.

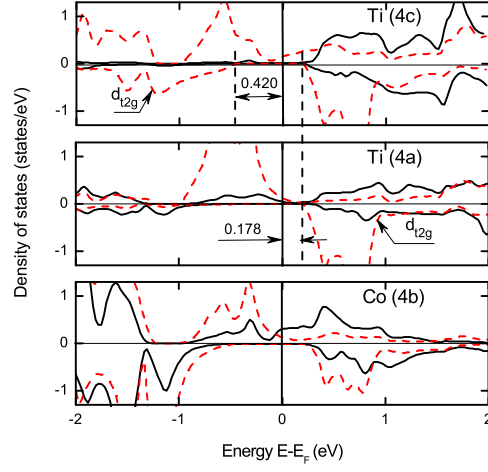


Figure 4: The main partial densities of states at optimized lattice parameter of  $Ti_2CoSn$ ,  $d_{eg}$  and  $d_{t2g}$  being indicated by solid and dashed line, respectively

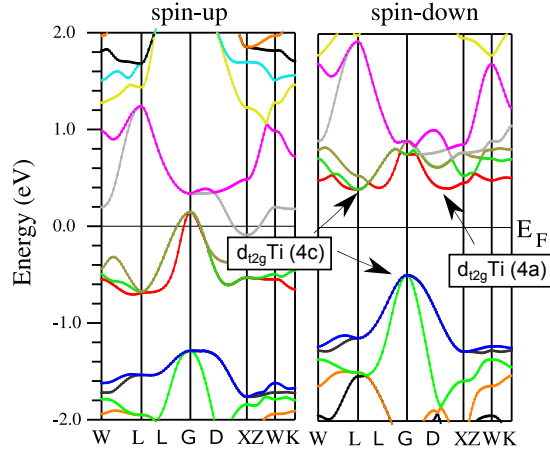


Figure 5: The band structure of  $Ti_2CoSn$  for spin-up (left panel) and spin-down (right panel) electrons for geometrical optimized structure

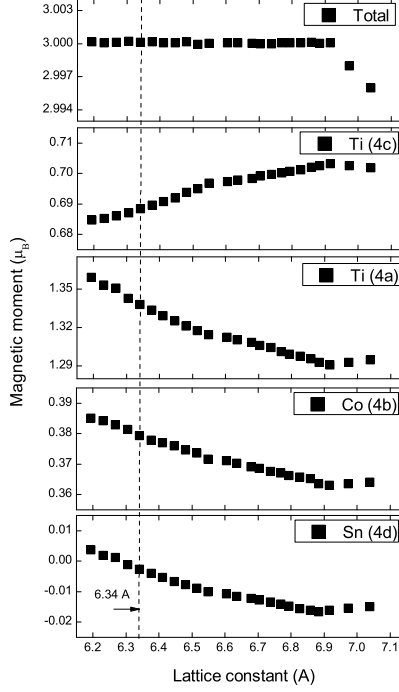


Figure 6: The total and site-specific magnetic moments of  $Ti_2CoSn$  compound as function of lattice constant.

reveal that the site-resolved magnetic moments per atom, at the optimized lattice constant are 0.918, 1.323, 0.177 and  $-0.0006 \mu_B$  for Ti(4c), Ti(4a), Co and Sn, respectively. A considerable contribution to the total magnetic moment comes from the interstitial region ( $0.582 \mu_B$ ).

The size of the band gaps as function of lattice parameter is displayed in Fig 7. The width of it decreases with the increase of lattice parameter. Furthermore, the more relaxed the structure become the Fermi level is shifted from the bottom edge of the minority conduction band to the upper edge of the minority valence band, which leads to a half metallic character for a lattice parameter up to 6.884 Å, when this property is lost and the  $Ti_2CoSn$  compound presents not only in majority but also in minority channel a clear metallic character.

In this context, the presence of energy gap in the minority spin channel leads to a 100% spin polarization for bulk  $Ti_2CoSn$ . The polarization remains constant for the lattice parameter interval where the compound has half metallic property, which makes the  $Ti_2CoSn$  an interesting material for future application in magnetoelectronics and spintronics.

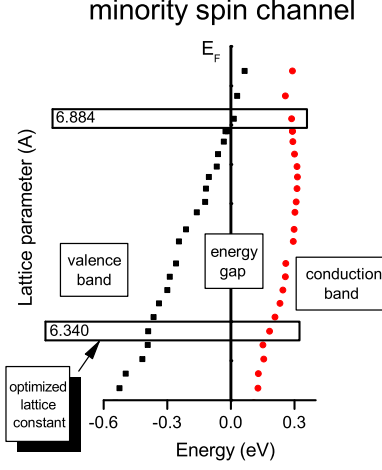


Figure 7: The positions of lowest unoccupied states from the conduction band (solid red circles) and of highest occupied states from valence band (solid black squares) of total DOSs from minority spin channel, for  $Ti_2CoSn$  as function of lattice parameter.

#### 4. CONCLUSIONS

The electronic band structure and magnetic properties of  $Ti_2CoSn$  were analyzed with the self-consistent full-potential linearized augmented-plane-wave basis scheme based on the density functional theory with the generalized gradient approximation (GGA). The results of spin-polarized calculations present the half-metallic ferromagnetic nature of  $Ti_2CoSn$  with a indirect band gap in the minority spin channel (0.589 eV) at calculated equilibrium lattice constant (6.340 Å). The magnetic moment of  $Ti_2CoSn$  material is  $3 \mu_B$ , fully polarized in a lattice parameter range of  $6.193 \div 6.884$  Å.

#### 5. ACKNOWLEDGMENTS

This work was financially supported from the projects PNII IDEI 75/2011 and Core Program PN09-450103 of the Romanian Ministry of Education Research, Youth and Sport.

#### References

- F. Heusler, W. Starck, E. Haupt, Verh DPG 5 (1903) 220.
- F. Heusler, Verh DPG 5 (1903) 219.
- P.G. van Engen, K.H.J. Bushow, R. Jongebreur, M. Erman, Appl Phys Lett 42 (1983) 202.



- R. Kainuma, Y. Imano, W. Ito, H. Morito, S. Okamoto, O. Kitakami, et al. Nature 439 (2006) 957.
- P.J. Webster, K.R.A. Ziebeck. Landolt-Brnstein e group III condensed matter, vol. 19C. Berlin: Springer (1988) 75.
- H.C. Kandpal, G.H. Fecher, C. Felser, J. Phys. D: Appl. Phys. 40 (2007) 1507.
- K.H.J. Buschow, P.G. van Engern, J. Magn. Magn. Mater. 25 (1981) 90.
- X.Q. Chen, R. Podloucky, P. Rogl, J. Appl. Phys. 100 (2006) 113901.
- K. Ramesh Kumar, J. Arout Chelvane, G. Markandeyulu, S.K. Malik, N. Harish Kumar, Solid State Commun. 150 (2010) 70.
- T.Graf, C. Felser, S.S. Parkin, Prog Solid State Ch 39 (2011)1
- R. Weht, W.E. Pickett, Phys. Rev. B 60 (1999) 13006.
- K. Ozdogan, I. Galanakis, E. Sasioglu, B. Atkas, J. Phys.: Condens. Matter 18 (2006) 2905.
- G. H. Fecher, Hem C. Kandpal, S. Wurmehl, and C. Felser, J. Appl. Phys. 99 (2006) 08J106.
- I. Galanakis, K. Ozdogan, E. Sasioglu, B. Aktas, Phys. Rev. B 75 (2007) 172405.
- Zhongyu Yao, Shaohua Gong, Jun Fu, Yue-Sheng Zhang, Kai-Lun Yao Solid State Commun. 150 (2010) 2239.
- H.Z. Luo, Z.Z. Zhu, L. Ma, S.F. Xu, H.Y. Liu, G.H.Wu, J. Phys. D: Appl. Phys. 40 (2007) 7121.
- J. Li, Y.X. Li, G.X. Zhou, Y.B. Sun, C.Q. Sun, Appl. Phys. Lett. 94 (2009) 242502.
- N. Kervan and S. Kervan, Intermetallics 24 (2012) 56
- Pugaczowa-Michalska Maria, Intermetallics 24 (2012) 128.
- N. Kervan and S. Kervan, Intermetallics 19 (2011) 1642.
- Lei Feng, Chengchun Tang, Shuangjin Wang, Wenchen He J. Alloys Compd. 509 (2011) 5187.
- S. Kervan and N. Kervan, Solid State Commun. 151 (2011) 1162.
- H.M. Huang, S.J. Luo, K.L. Yao, J. Magn. Magn. Mater. 324 (2012) 2560.
- Bayar E, Kervan N, Kervan S, J Magn Magn Mater 323 (2011) 2945.
- Kervan N, Kervan S, J Phys Chem Solids 72 (2011) 1358.

- Kervan N, Kervan S. J Magn Magn Mater 324 (2012) 645.
- Xiao-Ping Wei, Jian-Bo Deng, Ge-Yong Mao, Shi-Bin Chu, Xian-Ru Hu, Inter-metallics 29 (2012) 86.
- Zheng N, Jin Y. J Magn Magn Mater 324 (2012) 3099.
- P. Blaha, K. Schwarz, G. Madsen, D. Kvasnicka, J. Luitz, 2009 WIEN2k, An Augmented Plane Wave Plus Local Orbitals Program for Calculating Crystal Properties (Wien: Technische Universität Wien) <http://www.wien2k.at>
- J. P. Perdew, K. Burke, and M. Ernzerhof, Phys. Rev. Lett. 77 (1996) 3865.
- P.E. Blöchl, O. Jepsen, O.K. Andersen, Phys. Rev B 49 (1994) 16223.
- F.D. Murnaghan, Proc. Natl. Acad. Sci. USA 30(1944) 244.